EARTHQUAKE ENGINEERING AND STRUCTURAL DYNAMICS
Earthquake Engng. Struct. Dyn. **27**, 1503–1522 (1998)

FORMULATION OF ELASTIC EARTHQUAKE INPUT ENERGY SPECTRA

LUIS D. DECANINI*,† AND FABRIZIO MOLLAIOLI‡
Dipartimento di Ingegneria Strutturale e Geotecnica, Facoltà di Architettura, Università di Roma 'La Sapienza', Rome, Italy

SUMMARY

The object of this paper is to introduce a procedure for the determination of elastic design earthquake input energy spectra taking into account the influence of magnitude, soil type and distance from the surface projection of the fault. Firstly, an accurate selection of a large set of representative records has been realized. Secondly, the construction of the design input energy spectra has required determining the spectral shapes and a normalization factor which measures seismic hazard in terms of energy. This factor, denoted as the seismic hazard energy factor, has been defined as the area under the earthquake input energy spectrum in the period interval between 0·05 and 4·0 s. Finally, due to the importance of the source-to-site distance in the evaluation of the input energy, an investigation into the attenuation of the seismic hazard energy factor has been carried out. © 1998 John Wiley & Sons, Ltd.

KEY WORDS: input energy; seismic hazard energy factor; input energy attenuation

1. INTRODUCTION

The fundamental need to improve the reliability of the current procedures of earthquake-resistant design of structures has led to the recognition of methodologies based on energy criteria as effective tools for a comprehensive interpretation of the behaviour observed during recent destructive events. Energy-based design involves considering two essential aspects: the first is related to the establishment of Design Earthquakes, while the second concerns the evaluation of the actual energy absorption and energy dissipation capacities of structures.

The aim of this work is to introduce a proposal which could contribute to the resolution of the first of the above-mentioned aspects, namely the definition of a design seismic action as a function of appropriate parameters providing a measure of the energy actually transferred from soil to structures during seismic shaking.

The commonly adopted design approach in terms of forces, based on both elastic and inelastic response spectra, as results from the analysis and interpretation of the observed structural behaviour is open to criticism. The most controversial and uncertain aspect of the conventional design procedures specified by the different codes is represented by the interpretation of the elastic design spectrum as a measure of destructiveness and, by the definition of the elastic response reduction factor as a function of a presumed inelastic behaviour. This factor, also known as the behaviour factor, although it is based on the comparison between elastic and inelastic response spectra and non-linear structural analysis, is still substantially assigned by the codes according to empirical criteria. Furthermore, uncertainty often arises in various steps of these

* Correspondence to: Luis D. Decanini, Dipartimento di Ingegneria Strutturale e Geotecnica, Universita degli studi di Roma 'La Sapienza', via Antonio Gramsci, 53, 00197 Roma, Italia. E-mail: decanini@hp720.dsg.uniroma1.it
† Full Professor
‡ Ph.D

CCC 0098–8847/98/121503–20$17·50

Received 17 April 1997
Revised 10 February 1998

procedures because the inelastic spectra, obtained by adopting this methodology, do not contain the totality of the information necessary to characterize the damage potential. In this context, the introduction of appropriate parameters formulated in terms of energy might lead to more reliable predictions, since the concept of energy provides tools which allow to account more rationally for the mechanisms of generation, transmission and destructiveness of seismic actions.

An attempt to define an energy-based design procedure was made in 1956 by Housner.[1] However, this proposal has remained an isolated episode until the last decade, when the availability of a great quantity of records from severe earthquakes had determined a decisive impulse to researches on energy criteria. The contribution of Zahrah and Hall,[2] in 1984, and Akiyama,[3] in 1985, added to the renewal of interest in the design based on energy concepts. An improvement to the delineation of a methodology is owed to Uang and Bertero,[4] who derived the fundamental energy balance equations, and went on to examine and compare the features of the seismic energy input spectra obtained from different records. Further advancement in the introduction of energy parameters in the seismic verification is due to Fajfar *et al.*,[5,6] Nassar and Krawinkler,[7] and Lawson and Krawinkler.[8]

2. FORMULATION OF SEISMIC INPUT ENERGY SPECTRA: DELINEATION OF THE METHODOLOGY

The formulation of a design methodology in terms of energy is based on the premise that the energy transmitted by the design earthquake must be less than or equal to the energy absorption and dissipation capacities possessed by the structural system. The first difficulty connected with this approach derives from the necessity to predict the seismic input energy transmitted to the structures. The analyses of seismic input energy spectra found in literature, up to the time when the present study was being undertaken, has provided an indication of the noticeable variability in the significance and distribution of the energy transmitted to the structures. For example a perplexing circumstance was constituted by the recognition that seismic input energy spectra corresponding to earthquakes with more or less similar strength inelastic response spectra were very different from each other, as in the case of the records of Chile, 1985 and San Salvador, 1986.[9] Moreover, relationships between the earthquake input energy spectra and parameters such as magnitude, closest distance from the seismic source, soil type, focal mechanism, and so on, were not well known.

Many researches directed to the study of seismic actions have stressed the fact that the validity of results may be heavily conditioned by the choice of the strong ground motion records.[9,10] As a matter of fact, this aspect is crucial not only for assessing the reliability of the various indexes utilized in order to characterize the destructive power of earthquakes, but also and principally for the management of questions related to the definition of the earthquake input energy. Therefore, the need has emerged to perform an accurate selection of representative records, subsequently collected in a vast, appropriately built database. Prior to organizing this database was necessary to carry out a large amount of analysis of the whole set of available records. In accordance with the results of these preliminary studies, 296 records referred to ground motion horizontal components obtained during 37 seismic events have been selected and then classified according to *Magnitude*, *Soil type* and *Closest Distance from the surface projection of the fault rupture causative of the earthquake.*

In this paper, the elaboration of the energy spectral parameters has been referred to linear elastic Single-Degree-Of-Freedom (SDOF) systems. The definition of seismic input energy spectra for inelastic systems as well as the ratio of the energy dissipated through inelastic deformations to the input energy are discussed by Mollaioli.[11]

The definition of design input energy spectra requires determining not only the spectral shapes but also the scale factor representative of the destructive power of the expected ground motion. That is to say, it is necessary to identify a parameter which characterizes adequately the ground motion intensity, and which provides a complete description of the energy which can be transmitted to the different structures (such a parameter can therefore be seen as a substitute for the current seismic hazard parameters, such as PGA,

PGV, macroseismic intensity, and so on). To this purpose the proposed parameter is defined as the area of the earthquake input energy spectrum in the period interval between 0·05 and 4·0 s, indicated as AEI(0–4). As far as elastic systems are concerned, the definition of this parameter is accomplished by taking into account the influence of the magnitude, the soil type and the distance from the surface projection of the fault. The fact that the distance from the seismic source significantly affects the value of the input energy has demanded an accurate investigation into the problem of earthquake input energy attenuation.

Finally, once the design spectral shapes and the seismic hazard energy factor have been identified, it is possible to obtain the elastic design earthquake input energy spectra.

3. STRONG GROUND MOTION RECORDS SELECTION CRITERIA

Among the criteria behind the selection of earthquake ground motion records, the following can be mentioned: (a) the representativity of a wide set of cases characterized by different values of magnitude, distance to the causative fault, soil type, duration, etc.; (b) the knowledge of the earthquake damage scenarios corresponding to the location of the recording stations; (c) the spatial distribution of the strong ground motion records; and (d) the localization of the instruments.

The selected 296 records, taken from 37 seismic events, have been obtained over a period of time spanning from 1940 (Imperial Valley, El Centro) to 1995 (Kobe). The database contains time histories ranging from a magnitude $M_L = 4$ (Ancona, Italy, 1972) to a magnitude $M_S = 8{\cdot}1$ (Mexico, 1985), and whose distance from the causative fault ranges between 0 and 389 km. Table I represent the distribution of the records as a function of the type of soil which, as it will be shown in the following, has a considerable influence on the study of the energy aspects. The distribution of the records is not very uniform with respect to the magnitude, since the data are principally concentrated in the interval between 5·2 and 7·1. For the majority of the stations both the horizontal components have been considered. Most data are derived from records obtained from instrumental stations described as *free-field*, or located at ground level in small buildings (*one-storey buildings*).

4. DETERMINATION OF THE ENERGY PARAMETERS

Uang and Bertero[4] have derived the two basic energy equations namely the 'absolute' and the 'relative' energy equations. In this investigation the 'absolute' energy input has been considered, which for the numerical integration in the time domain for viscous damped SDOF systems can be written as

$$\frac{E_I}{m} = \int \ddot{u}_t \, du_g = \int \ddot{u}_t \dot{u}_g \, dt \tag{1}$$

where m is the mass, $u_t = u + u_g$ is the absolute displacement of the mass, and u_g is the earthquake ground displacement. From now on the input energy per unit mass, i.e. E_I/m, will be denoted as E_I. Then the energy balance equation can be written as follows:

$$E_I = E_k + E_\xi + E_a = E_k + E_\xi + E_s + E_H \tag{2}$$

Table I. Distribution of the records according the soil class

Soil type	S1 (rock)	S2 (intermediate)	S3 (soft)
no. of records	89	156	51

where E_k represents the absolute kinetic energy, E_ξ is the damping energy, and E_a is the absorbed energy that is composed of the recoverable elastic strain energy, E_s, and of the irrecoverable plastic hysteretic energy E_H.

As Uang and Bertero[4] have clearly stated, various reasons encourage one to investigate the absolute earthquake input energy. Anyway, it must be reported that Zahrah and Hall,[2] Kuwamura and Galambos,[12] Riddell[13] and Fajfar *et al.*,[14] have resorted to the relative energy in their studies. The alternative use of the absolute or the relative form of the energy significantly influences the deduced trends, particularly in the band of high frequencies, even though the maximum values of the energy demand (Seismic Input Energy) obtained in the two cases are very similar in the interval of periods between 0·3 and 5 s, as shown by Uang and Bertero.[4]

As mentioned before, in the present study the elastic input energy spectrum E_I for each of the 296 strong motion records has been calculated by considering the absolute energy equation. On account of the poor reliability of the corrected earthquake ground motions records beyond periods of 4 s, herein the spectra have been computed for fundamental periods between 0·05 and 4·0 s. Then the area enclosed by each of the elastic input energy spectra within the range of period 0·05–4·0 has been calculated. This parameter, denominated AEI(0-4), represents the seismic hazard energy factor. Furthermore, the maximum value of E_I and the corresponding period have been identified for each ground motion.

Regarding the damping, it must be pointed out that this parameter does not appear to have a significant influence on the magnitude of the seismic elastic input energy within the usual structural values. Furthermore, the following points should be stressed: (a) a quantitative definition of causes producing effects equivalent to a viscous damping in vibrating structures is not available yet; (b) it is difficult to evaluate the initial damage of the so-called non-structural elements; (c) it is well-known that damping depends on the structure deformation level; (d) when large deformations occur, as in the case of severe seismic events, it is often very difficult to distinguish experimentally the effects of the viscous damping from those of the inelastic behavior; (e) it is probable that the actual energy dissipation mechanisms are in fact much more complex than those of the simple viscous model adopted in the formulation of the fundamental equation of motion. According to the previous remarks, in order to study the seismic input energy it has been decided to choose a unique value for the viscous damping, namely 5 per cent of the critical value, representative of the average possessed by concrete and steel structures in the presence of non-structural elements, for deformation levels corresponding to severe seismic actions.

5. INFLUENCE OF THE EXTERNAL FACTORS ON THE INPUT ENERGY

Among the several external factors (magnitude or seismic moment, distance from the seismic source, focal mechanism, local soil conditions under the recording station, etc.) affecting the earthquake response, in what follows, a description of the principal parameters, which have been specifically considered in this study and have a relevant influence on the input energy will be found.

One of the main factors usually employed to describe the energy release at the seismic source is the *Magnitude* or the *Seismic Moment*. The magnitude values adopted in this study are referred to the local Richter magnitude M_L for values less than 6, and to the surface waves magnitude M_S for values equal to or greater than 6. This simplification makes sense in the light of the magnitude saturation phenomenon, associated with various magnitude scales, except with moment magnitude M_W. Unfortunately the data related to M_w are available only for recent earthquakes, while for events of the past it would have been necessary to have recourse to appropriate conversion laws, thus introducing further uncertainties. Preliminary observations on the magnitude influence have shown that the earthquake input energy, except for some specific events, does not continuously vary with the magnitude. However, taking the following magnitude intervals into account (a) $4{\cdot}2 \leqslant M \leqslant 5{\cdot}2$; (b) $5{\cdot}4 \leqslant M \leqslant 6{\cdot}2$; (c) $6{\cdot}5 \leqslant M \leqslant 7{\cdot}1$; and (d) $M > 7{\cdot}1$, it has been observed that E_I and AEI(0-4) tend to increase with the magnitude.

Generally it is possible to note that there is very little correlation between the epicentral distance and strong ground motion parameters, especially for records obtained from stations located in the proximity of the fault for which the point-source model is not valid. For this reason, *the closest distance from the surface projection of rupture* D_f has been chosen among the possible distance measures. Other measures, perhaps more meaningful, have not been considered due to lack of data. For the individualization of D_f, when the values were not available, it has been necessary to consider the focal mechanisms, the spatial distribution of the aftershocks, and the examination of the seismogenic zones in which the tectonic processes causing earthquakes have been identified. The influence of the source-to-site distance on the input energy spectra has been quantified by considering distance intervals. According to the available data, the following intervals have been chosen: (a) $D_f \leqslant 5$ km, characteristic of the near-fault area; (b) $5 < D_f \leqslant 12$ km, corresponding to sites where the effects due to the closeness of the seismic source can still be perceived; (c) $12 < D_f \leqslant 30$ km, relative to intermediate distances; (d) $D_f > 30$ km. This last wide interval, in which the attenuation is meaningful, remains open due to the lack of data.

The soil conditions in the site where the recorded stations are located has significant effects. Since the information found in the literature is often not exhaustive and is sometimes only referred to as surface geological layers, the classification in soil types has required the consideration of both acceleration and energy spectral shapes. The results so obtained have indicated the need to group the records according to three soil types denoted briefly as *rock or firm soil (S1), intermediate soil (S2), soft soil (S3)*. The multiplicity of both the soil features and the condition and depth (H) of different layers, has permitted to associate to the soil types, in addition to a general description, the approximate values of the shear wave velocity shown in Table II.

The frequency content of the ground motion time histories is worthy of some comments, since it affects the earthquake input energy, because the intensity and the variation of the transmitted energy with T depend upon the duration of the acceleration pulses. High-frequency pulses, which do not cause a significant damage to the buildings, lead to high spectral acceleration inconsistent with the corresponding moderate energy effectively imparted to the structures. On the contrary, if the duration of the pulses is high (low to medium frequencies), the corresponding input energy can reach considerable values, even though the acceleration intensity of the records is not particularly remarkable. These two effects are clearly expressed by the input energy spectra, especially when the influence of the source-to-site distance is taken into account. The acceleration time histories recorded near the causative fault generally show relatively large low-frequency pulses, which correspond to high incremental velocities. This kind of ground pulses, associated directly with the fault-rupture process and with the proximity of the seismic source, has been found for example in the near fault strong ground motion records of San Fernando (1971), Imperial Valley (1979), Northridge (1994) and Kobe (1995) events.

About 20 years ago, Bertero *et al.*[15] suggested that the long duration pulses, characteristic of the near-field record of Pacoima Dam (San Fernando, 1971), caused the severe damaging of the Olive View Hospital, rather than the high frequency and high intensity acceleration spikes (1g). Although some evidences indicate

Table II. Classification of soil conditions

Type	Profile	Shear wave velocity V_s (m/s)
S1	Rock	$\geqslant 700$
	Stiff Deposit $H < 50$ m	400–700
S2	Stiff Deposit $H > 50$ m	400–700
	Intermediate $H > 8$ m	100–400
S3	Soft soil deposits	< 100

that a thrust earthquake produces more severe ground motion than a strike-slip, the long duration pulses in the near-source area have been noticed for both focal mechanisms (e.g. Kobe 1995 and Northridge 1994).[16]

The presence of these near-fault distinctive low-frequency pulse-like time histories, different from other long-period motions such as those arising from soft-soil effects (e.g. Mexico, 1985), contributes significantly to the damage of the structures, because they result in a sudden burst of energy that must be dissipated immediately. The consequent deformation is characterized, generally, by one large yield excursion with few reversals. The above-mentioned effects, derived from the analysis of the acceleration and velocity time histories, are clearly identified by the input energy spectra, particularly, in the distance interval corresponding to 0–5 km.

In general, from the considerations summarized above and discussed in greater detail in Mollaioli,[11] the authors believe that the need to simultaneously take into account both the characteristics of earthquake ground shaking (such as amplitude, frequency content, strong ground motion duration, the sequence of the severe acceleration pulses) and the dynamic characteristics of the structures, in order to identify the damage potential of an earthquake at a given site, can be addressed by the use of input energy spectra (elastic and inelastic).

In conclusion, the study of the external factors affecting the earthquake input energy, permits one to quantify the influence of the magnitude, the distance to the source and the soil type.

6. NORMALIZATION CRITERIA FOR THE INPUT ENERGY SPECTRAL SHAPES

The problem of the establishment of a normalization criterion for the definition of design input energy spectral shapes, which is necessary to include seismic events of different severity, can be solved choosing between the two following methods:

(1) The normalization can be carried out directly on the acceleration records, before the dynamic analyses, by means of some ground motions parameters (PGA, etc.); the input energy spectra are determined in a successive phase, (14, 17)
(2) The normalization can be accomplished directly on the input energy spectra by choosing an appropriate scale factor that contemplates the values of E_I in the function of the dynamic characteristics of all structures that are of interest.

Although the first criterion allows parametric analyses in order to investigate the effects of some factors connected to the structural response, the influence of parameters such as magnitude, distance from the source and soil type cannot be detected.

On the other hand, the second criterion, operating on the E_I spectra directly, enables calibration and throws light on the effect of the external factors (M, D_f, soil type) governing the characteristics of the ground motion. Following this approach the definition of design actions in terms of energy can only be accomplished via a comprehensive and direct treatment of energy spectra on a statistically significant amount of data.

According to the second criterion, and using the whole set of E_I spectra, the search for spectral shapes and a scale factor characteristic of seismic hazard requires choosing a normalization procedure, in order to adequately grasp the trend of the phenomenon, and to minimize the possibility of deviations affecting the statistical manipulation.

The normalization procedure for the maximum input energy, $E_I(\max)$, considers as a reference, the maximum value of the input energy spectrum, generally corresponding to a narrow band of frequencies. This value therefore assumes a preponderant role, but it actually may not be representative of the general way in which the transmitted energy affects all the structures having $0{\cdot}05 < T \leqslant 4{\cdot}0$(s). As a matter of fact, trying to define seismic hazard as a function of a descriptive parameter bound to the maximum value only causes more consistent dispersion than other indexes adopted in the statistical analysis of spectral shapes.

Normalization of the input energy through the area enclosed by the spectrum itself has proved to constitute the most appropriate procedure to obtain design spectral shapes. The area used in the normalization, and also adopted as the seismic hazard energy factor, is that enclosed by the energy spectrum in the interval of periods between 0 and 4 s, AEI(0-4), expressed in cm^2/s and taking into account how the E_I varies as a function of the vibration period of the real structural systems. Dividing the spectral ordinates by AEI(0-4), a normalized spectrum expressed in s^{-1} (corresponding to a frequency) is obtained. The area of the normalized spectrum is equal to 1, and is dimensionless. Note that, in comparison with the normalization in terms of E_I(max), the shapes of the energy spectra normalized with respect to its area are smoothened. Furthermore, the area enclosed by the spectrum acts in a sense as a normalization weight for the spectral ordinates, as it allows to account more adequately for the variations as a function of the periods. A further aspect contributing to the choice of this criterion is constituted by the greater statistic stability, highlighted by the minor variation coefficients resulting from the use of the areas as a normalization factor.

7. LINEAR ELASTIC SPECTRAL SHAPES

The elastic spectral shapes have been obtained by dividing the ordinates of the input energy spectrum by the corresponding value of AEI(0-4).

7.1. Influence of the soil type

After grouping the strong ground motion records according to three different soil types, S1, S2, and S3, the corresponding spectral shapes have been evaluated; the values have then been statistically analysed, following the hypothesis that the ordinates of the spectrum, for an assigned period, are normally distributed.

The importance of the distinction in soil types is clearly highlighted in Figure 1, which shows the mean spectral shapes as a function of the soils S1, S2, and S3, including all distance and magnitude values. As it can be seen, the three spectral shapes are significantly different from one another. The maximum values are close to 1, for soil S1, 0·7 for S2, and close to 0·4 for soil S3, and correspond to different periods of vibrations, 0·20, 0·40-0·45, and 0·95 s, respectively, for the soil S1, S2 and S3.

A remarkable feature of the spectral shapes, in contrast with the typical characteristics of the pseudoacceleration spectra, is represented by the notable difference in the maximum values observed in the energy spectral shapes which is a consequence of the adopted normalization procedure. In fact, if the normalization is performed using for each accelerogram the maximum value of E_I, the peak values of the above spectra appear to be slightly differentiated, so that the resulting spectral shapes do not clearly show the effect of the soil. Figure 1 also shows the basically linear trend of the spectral shape corresponding to periods ranging from 0·05 s to the value associated to the maximum ordinate for the three types of soil.

From the values of the variation coefficients (VC), shown in Figure 2, it can be recognized that the dispersion is generally considerable, though compatible with that encountered when using the parameters currently adopted in the characterization of the ground motion. For very high frequencies, soils S1 and S2 present a remarkable dispersion, which once again reveals the presence of the uncertainty strongly affecting this band of periods.

7.2. Influence of the distance to the causative fault

With the aim of investigating the influence of the distance D_f to the source on the spectral shapes, records in the data-set have been grouped according to three different intervals of distance, appropriately selected to rely on a sufficiently high number of records corresponding to each interval. The peak values of the spectral shapes and the corresponding periods T_{pk} (in s), for 4 distance intervals (in km), are indicated in Table III.

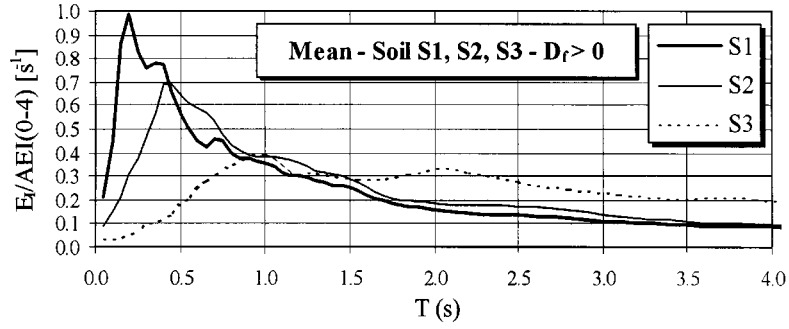

Figure 1. Mean energy spectral shapes in function of soil S1, S2, S3

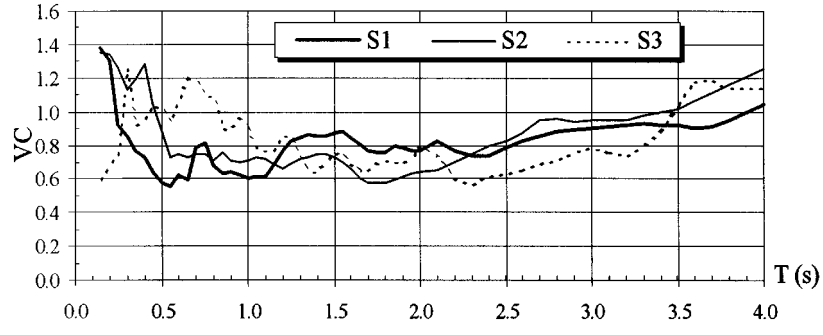

Figure 2. Variation coefficients (VC) of elastic input energy spectral shape. Soils S1, S2, and S3

Table III. Effect of distance on the peak value E_I/AEI(0-4) (s^{-1}) and the corresponding period T_{pk} (s)

	S1		S2		S3	
D_f (km)	T_{pk}	E_I/AEI(0-4)	T_{pk}	E_I/AEI(0-4)	T_{pk}	E_I/AEI(0-4)
$0 \leqslant D_f \leqslant 5$	0.18	0·98	0·40–0·45	0·68	0·80	0·40
$12 \leqslant D_f \leqslant 30$	0·20	1·08	0·40	0·86	1·85	0·47
$D_f > 30$	0·15	0·96	0·65	0·81	0·95	0·53
$D_f > 0$	0·20	1·00	0·40–0·45	0·70	0·95	0·40

As far as the soil S1 is concerned, both the period T_{pk} and the corresponding peak value remain practically unchanged. In soil S2 a certain effect of the distance can be noticed, mostly when D_f is greater than 30 km. This fact is reflected by a shift in T_{pk}, which has the value of about 0·65 s. The maximum ordinate value, on the other hand, does not vary significantly, ranging between 0·68 and 0·86. Finally, changes become evident for soil S3; nevertheless, they do not display trends defined clearly enough to agree with the specification of spectral shapes differentiated according to the distance. It may be interesting to note that a linear pattern up to T_{pk} constitutes a valid approximation in the case of differentiation of spectral shapes as a function of D_f, too.

7.3. *Influence of the magnitude*

The analysis of the effect of the magnitude on the spectral shapes has been carried out considering the four intervals of magnitude, indicated in Section 5, for each class of soil. The results are shown in Table IV.

For soil S1 and $4{\cdot}2 \leqslant M \leqslant 5{\cdot}2$, a considerably high value of the maximum ordinate of the spectral shape can be detected at $T_{pk} = 0{\cdot}2$ s; this value is about 3·6 times greater than the mean value ($M > 4$ in Table IV), and decays rapidly with increasing periods. Records corresponding to this interval (e.g. Ancona, 1972, and Bear Valley, 1972) are characterized by high PGA, very short duration, low-energy content and consequently low damage potential, with extremely selective effects in the range of high frequencies. Then, for soil S1 and $5{\cdot}4 \leqslant M \leqslant 6{\cdot}2$, both the peak value and T_{pk} seem close to the mean values ($M > 4$); the same can be stated in general for the whole spectral shape. The subsequent interval, i. e. $6{\cdot}5 \leqslant M \leqslant 7{\cdot}1$, shows a significant shift in T_{pk} towards the range of low frequencies, together with a reduction in the maximum spectral ordinate. Regarding magnitudes greater than 7·1, as previously pointed out, an inverse tendency is observed, yielding to values still closer to the general mean trend ($M > 4$).

Concerning the soil S2, a phenomenon analogous to that described for the lower magnitudes occurs, although with energy concentrated in a band of periods around 0·4 s. For the interval of magnitude ranging from 6·5 to 7·1, a shift in T_{pk} towards the band of low frequencies (0·65 s) can be observed once again, with a 65% reduction of the peak ordinate with respect to the mean value ($M > 4$ in Table IV). A shift in T_{pk} also occurs at $M > 7{\cdot}1$, while the maximum spectral value approaches the mean ($M > 4$).

Finally no data are available for the lower interval of magnitude in soil S3, while for $5{\cdot}4 \leqslant M \leqslant 6{\cdot}2$ the number of records is very small. In this interval the spectral ordinates concentrate around the period 0·7, with a peak as high as three times the mean value ($M > 4$). Regarding $6{\cdot}5 \leqslant M \leqslant 7{\cdot}1$, the trend follows the mean ($M > 4$), while at higher magnitudes a marked shift of T_{pk} appears (2·1 s); anyway it must be noted that this interval is strongly influenced by the record of Mexico City, 1985.

It can be concluded that the most remarkable trend is represented by the shift of T_{pk} toward the band of low frequencies, as the magnitude increases. This tendency becomes more noticeable as the stiffness of the soil decreases, and could be ascribed to a growth of the lower frequency components of the soil as the duration increases. Although the magnitude has not been included directly in the definition of the design spectral shapes, it is possible to take its effects into account by an adequate identification of the spectrum *plateau*. The intense energy concentration in correspondence with narrow bands of frequency detected at the lower magnitude interval has been included in the model by means of the seismic hazard energy factor.

8. LINEAR ELASTIC DESIGN SPECTRAL SHAPES

8.1. *Proposed analytical expressions*

The design spectral shapes should be associated with simple mathematical expressions and smoothened curves which eliminate non-meaningful local effects due to specific singularities in the ground motion.

Table IV. Effect of magnitude on peak value of E_I/AEI(0-4) (s^{-1}) and the correspondent period T_{pk} (s)

	S1		S2		S3	
M	T_{pk}	E_I/AEI(0-4)	T_{pk}	E_I/AEI(0-4)	T_{pk}	E_I/AEI(0-4)
$4{\cdot}2 \leqslant M \leqslant 5{\cdot}2$	0·20	3·60	0·40	3·60	—	—
$5{\cdot}4 \leqslant M \leqslant 6{\cdot}2$	0·15	1·11	0·45	1·00	0·70	1·25
$6{\cdot}5 \leqslant M \leqslant 7{\cdot}1$	0·40	0·68	0·65	0·47	0·95	0·47
$M > 7{\cdot}1$	0·30	0·98	0·70	0·77	2·10	0·48
$M > 4$	0·20	1·00	0·40–0·45	0·70	0·95	0·40

Furthermore, such shapes should reflect the various trends identified in the course of the analysis and that have been previously discussed.

The influence of the type of soil has proved to be essential, and thus its explicit inclusion in the formulation of the design spectral shapes has been considered indispensable. On the other hand, though significant effects of both the distance and the magnitude has been observed, it has not been possible to quantify and characterize their effects in a manner satisfactory enough to include them directly in the analytical model; nevertheless the observed trend has been taken into account in the phase of defining of the obtained shapes.

Let f_E denote the energy spectral ordinate representing the ratio of the input energy E_I (per unit mass) and the seismic hazard energy factor, it can be written as

$$f_E = \frac{E_I}{\text{AEI(0-4)}} \ (\text{s}^{-1}) \tag{3}$$

The following functional relation can be specified:

$$f_E = f(T; S; \xi) \tag{4}$$

where T is the vibration period, S is the class of soil; ξ is the viscous damping coefficient assumed as 5 per cent. The fundamental shape that has been chosen for f_E is shown in Figure 3.

It consists of three different relations: a linear variation for the lower periods; a constant region in the intermediate band of periods; and a decreasing curve in the zone of the higher periods.

The above three regions are respectively characterized by the following equations:

$$\begin{aligned} &T_0 \leqslant T \leqslant T_1\text{: } f_E = a + (b-a)\frac{T - T_0}{T_1 - T_0} \\ &T_0 \leqslant T \leqslant T_1\text{: } f_E = b \qquad (f_E \text{ in } \text{s}^{-1}) \\ &T \geqslant T_2\text{: } f_E = b\left(\frac{T_2}{T}\right)^k \end{aligned} \tag{5}$$

The parameters a, b, T_1, T_2 and k depend on the soil type: 'a' represents the normalized spectral ordinate corresponding to the lower considered period, 0·05 s (T_0); 'b' is the maximum spectral value relative to the constant value of the spectrum; T_1 is the period corresponding to the beginning of the constant value of the spectrum (referring to the mean of the data set, this value is approximately coincident with the dominant period of the soil for class S2, while it is lower than the dominant periods in both soils S1 and S3);

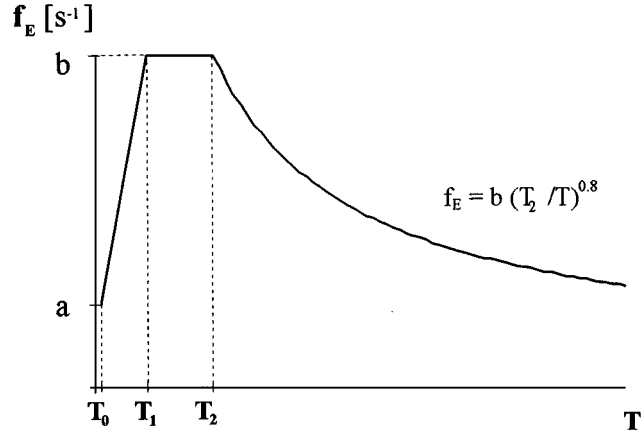

Figure 3. Elastic design input energy spectral shape

T_2 represents the period at which the decreasing branch starts; 'k' is a parameter governing the decay, and it is assumed to have the same value for the three classes of soil, according to the indications that emerged from the analyses.

The values of the parameters introduced above are given in Table V, together with the area enclosed by the design spectral shape $\text{SSA(0-4)}_{\text{design}}$, which is greater than unity. In fact, $\text{SSA(0-4)}_{\text{design}}$ constitutes the envelope of all the spectral shapes, corresponding to each record, which instead have areas equal to 1.

8.2. Comparison with recorded data and discussion on the proposal of design spectral shapes

The design spectral shapes have been compared with the mean and with the mean plus a standard deviation (SD) spectra, considering all the magnitudes and distances from the source intervals, for each class of soil, as illustrated in Figure 4.

As it can be noticed, the spectral shapes always cover the mean values, while in the low frequency region they are exceeded by the means plus a SD. Except soil S3, for which significant dispersions occur, the decaying branch of the design spectrum accurately fits the analogous portion of the curve relative to the mean plus a SD spectrum.

Both the distance and the magnitude do not affect the design spectral shapes directly. Nevertheless, for a given site, combining the spectral shape with the seismic hazard energy factor, which is a function of both magnitude and distance, a site specific design input energy spectrum can be obtained.

The proposed spectral shapes do not present a uniform exceedence probability for the different vibration periods. Attempts at developing isoprobable spectral shapes lead to quite irregular patterns, which can hardly be approximated with simple analytical expressions. It should also be remarked that the isoprobability criterion becomes less meaningful as the effects of magnitude and distance are not directly included in the model.

Despite the intrinsic limitation of this concept, the meaning of a 70 per cent percentile can be assigned on average to the proposed spectral shapes, taking account of the entire interval of periods and the three different soils.

9. SEISMIC HAZARD ENERGY FACTOR

The need to identify a parameter which characterizes adequately the damage potential of the expected ground motion, fully describing the distribution of the energy imparted to the different structures, has led to the recognition of a seismic hazard energy factor, denoted as AEI(0-4), which has been obtained by adopting the area enclosed by the input energy spectrum in the interval of periods between 0·05 and 4·0 s. Combining the spectral shape with the seismic hazard energy factor AEI(0-4), the maximum input energy $E_{\text{I}}(\max)$ can be determined as:

$$E_{\text{I}}(\max) = b\ \text{AEI(0-4)} \tag{6}$$

with b equal to 1, 0·8, and 0·6 (see Table V), respectively, for the soils S1, S2, and S3.

Table V. Values of the parameters introduced in Figure 2 for the soil S1, S2 and S3

Soil	a	b	T_1	T_2	k	$\text{SSA(0-4)}_{\text{design}}$
S1	0·30	1·00	0·10	0·50	0·80	1·720
S2	0·20	0·80	0·40	0·90	0·80	1·830
S3	0·10	0·60	0·70	2·20	0·80	1·966

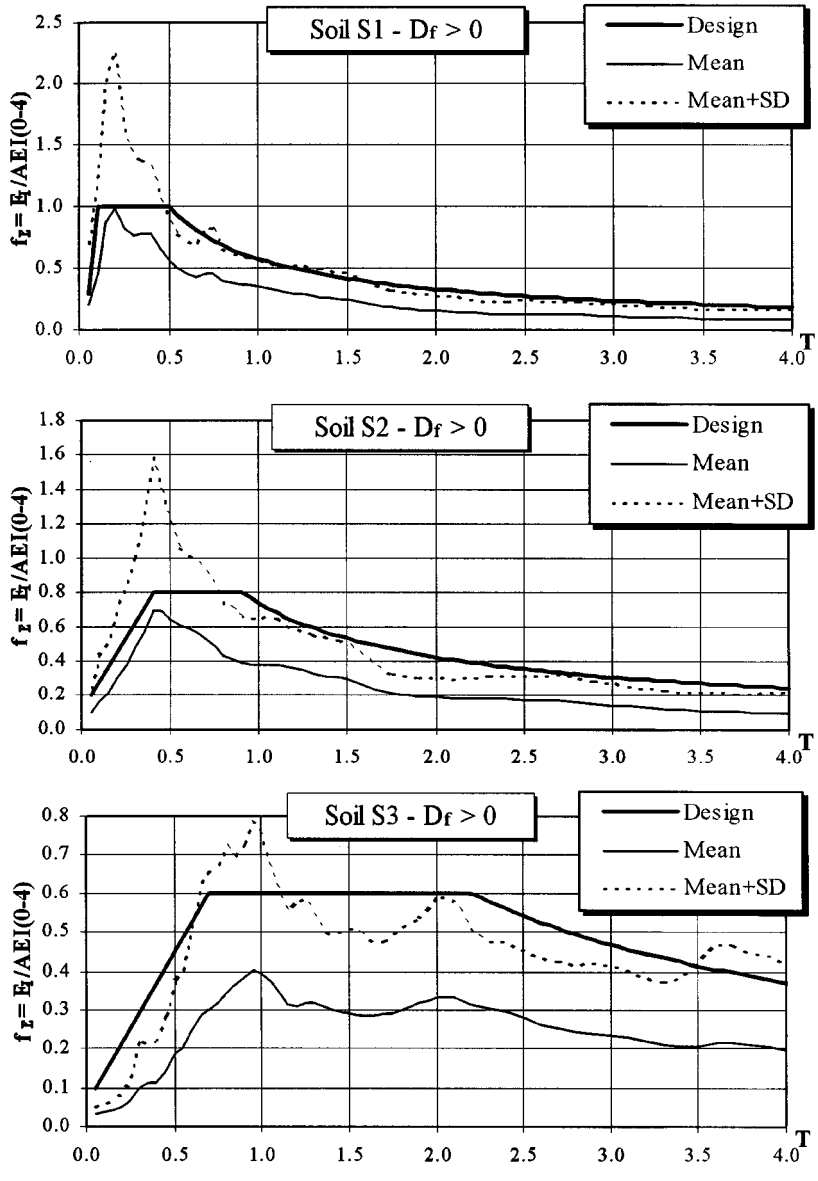

Figure 4. Comparison of the design spectral shapes, the mean spectra and the mean plus one standard deviation spectra relative to all accelerometric records according to the soil type (s^{-1})

As already discussed, it is not possible, at the moment, to quantify all the factors affecting the intensity and the spectral distribution of the input energy. For this reason the seismic hazard energy factor has been defined according to the source-to-site distance intervals, soil types, and magnitude intervals indicated in Section 5. The complexity of the seismic hazard energy factor definition as a function of the above-mentioned parameters is due to: (a) lack of reliable attenuation relationships of AEI(0-4) and E_I; (b) poor correlation between E_I(max) and the several index characteristics of the damage potential of the ground motion

(Housner intensity, Arias intensity, etc.); (c) unsatisfactory results of the regressions carried out on the values of $E_I(\max)$ as a function of the magnitude, distance and soil type. In an attempt to cope with these difficulties, an iterative and feedback process based on the obtainable information on areas AEI(0-4) and the trend of the relative attenuations has been followed.

Firstly, the area AEI(0-4) and $E_I(\max)/b$ values (obtained from the single available records) have been grouped in classes according to soil types, magnitude intervals, and source-to-site distance D_f intervals. From the resulting 39 classes, 21 have a number of data equal to or greater than 4 values (8 classes for soil S1, 9 for soil S2, and 4 for soil S3), 11 classes do not have any data, and 7 classes have a number of data less than 4.

In the first phase, mean values, mean values plus the standard deviations, peak values of AEI(0-4), and $E_I(\max)/b$, have been taken into account. Combining these values with the corresponding spectral shapes an initial version of the design seismic input energy spectrum was developed. The establishment of the preliminary design values of AEI(0-4) has been guided by the consideration of data relevant to specific representative cases and the observed trend of the attenuation.

Secondly, the spectra obtained in the first phase were compared with each of the corresponding specific spectra. The values of the seismic hazard energy factors have then been gradually modified so that the ordinates of the design spectra are generally not exceeded by those of the different records (except in some exceptional cases). Besides, the consistency of the resulting values has been checked through the various iteration steps examining the correlations available as a function of the different parameters. The values of the design seismic hazard energy factor derived by this procedure are reported in Table VI.

Finally, a statistical analysis has been conducted only for the classes having a number of data equal to or greater than 4. The principal results are illustrated in Table VI, where the design AEI(0-4) values, derived from the elaborations, are compared with the statistical values of AEI(0-4) and $E_I(\max)/b$ obtained from the records included in the data set, by means of the variation coefficients VC and the percentiles (n represents the number of records contained in each classes). The areas AEI(0-4) and $E_I(\max)/b$ values control the spectral distribution and the plateau of the design spectrum respectively.

A fundamental criterion adopted for the establishment of the seismic hazard energy factors is derived from the constraint that the design input energy spectra has a probability of exceedence of approximately 0·3–0·35. In order to reach this target, and on account of the fact that a statistical meaning of a 70 per cent percentile may be associated with the design spectral shapes, the design areas AEI(0-4) should have a lower probability of exceedence, corresponding to a percentile not less than 90 per cent.

The variation coefficients (VC) of AEI(0-4) values are mostly within the range 0·4–1·1 with a mean value corresponding to all classes equal to 0·79. The coefficients of variation of energy parameters are larger than those in the case of the 'classical' response parameters used for scaling of the ground motion, due to the fact that energies are proportional to the square of the 'classical scaling' parameters.

Moreover, the identification of the design seismic hazard energy factors AEI(0-4) has also been based on the following criteria:

(a) The design input energy spectrum should not be exceeded by the energy spectra corresponding to the strong motion records, except in some particular cases. This criterion gives a first indication on the envelope peculiarity of the design spectra.
(b) Grouping data according to soil types, magnitude intervals, and source-to-site distance D_f intervals, implies that some classes may have few data. In this case, the design AEI(0-4) values have been derived principally from the attenuation relationships.
(c) Classes with most data are considered to have more weight.
(d) The design seismic hazard energy factor should not be less than 85 per cent of the maximum value of AEI(0-4) and $E_I(\max)/b$.

Table VI. Comparison between design AEI(0-4) (cm^2/s) and experimental values of AEI(0-4)and E_I(max)/b

	Soil S1			AEI(0-4)		E_I(max)/b	
Magnitude	D_f (km)	n	Design AEI(0-4)	VC	Percentile	VC	Percentile
$4{\cdot}2 \leqslant M \leqslant 5{\cdot}2$	$D_f \leqslant 5$	2	6000				
$4{\cdot}2 \leqslant M \leqslant 5{\cdot}2$	$5 \leqslant D_f \leqslant 12$	4	2000	1·13	87%	0·43	96%
$4{\cdot}2 \leqslant M \leqslant 5{\cdot}2$	$12 \leqslant D_f \leqslant 30$	3	1600				
$4{\cdot}2 \leqslant M \leqslant 5{\cdot}2$	$D_f > 30$		600				
$5{\cdot}4 \leqslant M \leqslant 6{\cdot}2$	$D_f \leqslant 5$	8	15 000	1·02	> 99%	1·18	> 99%
$5{\cdot}4 \leqslant M \leqslant 6{\cdot}2$	$5 \leqslant D_f \leqslant 12$	12	4500	0·61	98%	0·91	97%
$5{\cdot}4 \leqslant M \leqslant 6{\cdot}2$	$12 \leqslant D_f \leqslant 30$	15	1800	0·74	> 99%	0·78	> 99%
$5{\cdot}4 \leqslant M \leqslant 6{\cdot}2$	$D_f > 30$	2	800				
$6{\cdot}5 \leqslant M \leqslant 7{\cdot}1$	$D_f \leqslant 5$	8	65 000	0·91	70%	0·65	
$6{\cdot}5 \leqslant M \leqslant 7{\cdot}1$	$5 \leqslant D_f \leqslant 12$	2	30 000				
$6{\cdot}5 \leqslant M \leqslant 7{\cdot}1$	$12 \leqslant D_f \leqslant 30$	14	16 000	0·60	99%	1·07	99%
$6{\cdot}5 \leqslant M \leqslant 7{\cdot}1$	$D_f > 30$	6	6000	0·70	81%	0·37	> 99%
$M \geqslant 7{\cdot}2$	$D_f > 30$	10	30 000	0·93	93%	1·27	98%
	Soil S2			AEI(0-4)		E_I(max)/b	
Magnitude	D_f (km)	n	Design AEI(0-4)	VC	Percentile	VC	Percentile
$4{\cdot}2 \leqslant M \leqslant 5{\cdot}2$	$D_f \leqslant 5$		16 000				
$4{\cdot}2 \leqslant M \leqslant 5{\cdot}2$	$5 \leqslant D_f \leqslant 12$	4	6000	0·37	> 99%	0·55	89%
$4{\cdot}2 \leqslant M \leqslant 5{\cdot}2$	$12 \leqslant D_f \leqslant 30$	2	2500				
$4{\cdot}2 \leqslant M \leqslant 5{\cdot}2$	$D_f > 30$		1000				
$5{\cdot}4 \leqslant M \leqslant 6{\cdot}2$	$D_f \leqslant 5$	21	45 000	0·90	92%	0·81	99%
$5{\cdot}4 \leqslant M \leqslant 6{\cdot}2$	$5 \leqslant D_f \leqslant 12$	10	18 000	0·76	> 99%	0·76	98%
$5{\cdot}4 \leqslant M \leqslant 6{\cdot}2$	$12 \leqslant D_f \leqslant 30$	21	10 000	1·04	> 99%	0·94	> 99%
$5{\cdot}4 \leqslant M \leqslant 6{\cdot}2$	$D_f > 30$	2	3000				
$6{\cdot}5 \leqslant M \leqslant 7{\cdot}1$	$D_f \leqslant 5$	22	110 000	0·62	82%	0·68	> 99%
$6{\cdot}5 \leqslant M \leqslant 7{\cdot}1$	$5 \leqslant D_f \leqslant 12$	20	75 000	0·50	> 99%	0·86	> 99%
$6{\cdot}5 \leqslant M \leqslant 7{\cdot}1$	$12 \leqslant D_f \leqslant 30$	33	50 000	0·73	97%	0·66	> 99%
$6{\cdot}5 \leqslant M \leqslant 7{\cdot}1$	$D_f > 30$	8	15 000	0·60	90%	0·51	> 99%
$M \geqslant 7{\cdot}2$	$D_f > 30$	10	110 000	0·67	97%	0·80	94%
	Soil S3			AEI(0-4)		E_I(max)/b	
Magnitude	D_f (km)	n	Design AEI(0-4)	VC	Percentile	VC	Percentile
$4{\cdot}2 \leqslant M \leqslant 5{\cdot}2$	$D_f \leqslant 5$		25 000				
$4{\cdot}2 \leqslant M \leqslant 5{\cdot}2$	$5 \leqslant D_f \leqslant 12$		12 000				
$4{\cdot}2 \leqslant M \leqslant 5{\cdot}2$	$12 \leqslant D_f \leqslant 30$		6000				
$4{\cdot}2 \leqslant M \leqslant 5{\cdot}2$	$D_f > 30$		3000				
$5{\cdot}4 \leqslant M \leqslant 6{\cdot}2$	$D_f \leqslant 5$		70 000				
$5{\cdot}4 \leqslant M \leqslant 6{\cdot}2$	$5 \leqslant D_f \leqslant 12$	3	40 000				
$5{\cdot}4 \leqslant M \leqslant 6{\cdot}2$	$12 \leqslant D_f \leqslant 30$		20 000				
$5{\cdot}4 \leqslant M \leqslant 6{\cdot}2$	$D_f > 30$		10 000				
$6{\cdot}5 \leqslant M \leqslant 7{\cdot}1$	$D_f \leqslant 5$	10	180 000	0·63	64%	0·76	98%
$6{\cdot}5 \leqslant M \leqslant 7{\cdot}1$	$5 \leqslant D_f \leqslant 12$		140 000				
$6{\cdot}5 \leqslant M \leqslant 7{\cdot}1$	$12 \leqslant D_f \leqslant 30$	10	100 000	0·85	88%	1·15	92%
$6{\cdot}5 \leqslant M \leqslant 7{\cdot}1$	$D_f > 30$	20	55 000	0·90	81%	0·75	98%
$M \geqslant 7{\cdot}2$	$D_f > 30$	8	180 000	0·47	50%	0·65	47%

10. EARTHQUAKE INPUT ENERGY ATTENUATION

10.1. Analysis of the entire data set

In this section the variation of the earthquake input energy as a function of the shortest distance from the surface projection of the causative fault, D_f is examined. The study of the attenuation of the area of the E_I spectra, considering the complete database, has been faced by grouping the data according to the soil classes and the magnitude intervals.

Table VII indicates the relative attenuation values R, representing the ratio of the mean value of AEI(0-4) corresponding to a definite source-to-site distance, to the mean AEI(0-4) relative to the proximity of the fault. The values of AEI(0-4) corresponding to D_f less than 5 km are considered as the source reference values. As it may be noticed, for $6{\cdot}5 < M < 7{\cdot}1$, the attenuation rate decreases passing from soil S1 to soil S3. In other words, the attenuation is lower as the soil stiffness decreases. This aspect is not confirmed for the interval $5{\cdot}4 < M < 6{\cdot}2$, for which the available data are referred to soils S1 and S2.

From the adopted values of the design seismic hazard energy factor the relative attenuation coefficients R have been obtained, as indicated in Table VIII.

As it can be seen, the design relative attenuation almost conforms to the trends specified by the previous analysis.

10.2. Comparison with the attenuation relationships of the ground motion parameters

The functional form of the attenuation equation of the maximum values of ground motion parameters is usually written as follows.[18]

$$\log y = a + b\,M + c \log D_e + dD_e + eS \tag{7}$$

where y is the ground motion parameter of interest (PGA or PGV), D_e is some distance from the earthquake source (epicentral, hypocentral, nearest distance to the rupture, etc.), M is the magnitude, S is a variable dependent on the soil class, and a, b, c, d and e are the regression coefficients that are independent of the magnitude, the distance from the source and the soil type. The relative attenuation R_y, indicated by the ratio of the y value at a certain distance from the source to that of the source:

$$R_y = \frac{Y_{D_e}}{Y_{\text{source}}} \tag{8}$$

Table VII. Relative attenuation of mean AEI(0–4) for all the available records

		SOIL S1	SOIL S2	SOIL S3
	1	1	1	$6{\cdot}5 < M < 7{\cdot}1$
$D_f < 5$	1	1	1	$5{\cdot}4 < M < 6{\cdot}2$
	1	1	1	$4{\cdot}2 < M < 5{\cdot}2$
	0·544	0·370		$6{\cdot}5 < M < 7{\cdot}1$
$5 < D_f < 12$	0·687	0·286		$5{\cdot}4 < M < 6{\cdot}2$
	0·700			$4{\cdot}2 < M < 5{\cdot}2$
	0·123	0·302	0·388	$6{\cdot}5 < M < 7{\cdot}1$
$12 < D_f < 30$	0·138	0·129		$5{\cdot}4 < M < 6{\cdot}2$
	0·191			$4{\cdot}2 < M < 5{\cdot}2$
	0·084	0·119	0·242	$6{\cdot}5 < M < 7{\cdot}1$
$D_f > 30$	0·170	0·032		$5{\cdot}4 < M < 6{\cdot}2$
				$4{\cdot}2 < M < 5{\cdot}2$

Table VIII. Relative attenuation of the design seismic hazard energy factor

	SOIL S1	SOIL S2	SOIL S3	
	1	1	1	$6{\cdot}5 < M < 7{\cdot}1$
$D_f < 5$	1	1	1	$5{\cdot}4 < M < 6{\cdot}2$
	1	1	1	$4{\cdot}2 < M < 5{\cdot}2$
	0·460	0·680	0·780	$6{\cdot}5 < M < 7{\cdot}1$
$5 < D_f < 12$	0·300	0·400	0·570	$5{\cdot}4 < M < 6{\cdot}2$
	0·330	0·375	0·480	$4{\cdot}2 < M < 5{\cdot}2$
	0·246	0·450	0·560	$6{\cdot}5 < M < 7{\cdot}1$
$12 < D_f < 30$	0·120	0·220	0·290	$5{\cdot}4 < M < 6{\cdot}2$
	0·270	0·160	0·240	$4{\cdot}2 < M < 5{\cdot}2$
	0·090	0·140	0·305	$6{\cdot}5 < M < 7{\cdot}1$
$D_f > 30$	0·050	0·070	0·140	$5{\cdot}4 < M < 6{\cdot}2$
	0·100	0·060	0·120	$4{\cdot}2 < M < 5{\cdot}2$

is neither dependent on the coefficient a, b, e, nor on M and S, being:

$$\log R_y = c[\log D_e - \log D_e(\text{source})] + d[D_e - D_e(\text{source})] \tag{9}$$

On the contrary, it may be noted from the results obtained by the analyses performed both on specific seismic events and the entire data set, that the relative attenuation of the parameter AEI(0-4) is a function of the soil class and the magnitude interval. As a matter of fact the regressed attenuation relationships determined using the equation (7) have led to unsatisfactory results for the following reasons: the regression coefficient a, b, c, d, and e do not depend on the soil class and the magnitude interval and the relation between magnitude and AEI(0-4) is represented by a step function. Owing to these considerations, another energy propagation model, adopted by Ambraseys[19] for his study on the attenuation of macroseismic intensity, has been utilized with some modifications. Therefore, the relative attenuation relationship of AEI(0-4) becomes:

$$R(\text{AEI}) = \frac{\text{AEI}_{D_f}}{\text{AEI}^*_{\text{source}}} = \frac{e^{-K_1 D_f}}{K_2 D_f^{K_3}} \tag{10}$$

or

$$\ln R(\text{AEI}) = \ln \frac{1}{K_2} - K_1 D_f - K_3 \ln D_f \tag{11}$$

where $\text{AEI}_{\text{source}}$ is the area at the source, and is the area at a distance D_f from the source. The coefficients K_1, K_2 and K_3 depend on the soil class and the magnitude interval. Ordering the available data by the type of soil and the interval of magnitude, and considering the mean values of AEI(0-4), the regressions yield the values of the coefficients $\ln(1/K_2)$, K_1 and K_3 reported in Table IX.

10.3. Comments on the size and attenuation of seismic input energy

The space variation of the seismic input energy and the associated seismic hazard energy factor constitutes a very complex phenomenon influenced by a number of factors. Given the variety and amount of the parameters involved, often interrelated, and considering the information and data available at present, it is not deemed convenient to rationalize this phenomenon resorting to a unique mathematical model, though multivariate, providing the desired reliability.

As expected, for a fixed D_f both the maximum seismic input energy, $E_I(\max)$, and the seismic hazard energy factor, AEI(0-4), increase with the magnitude. Nevertheless this trend is not continuous, since it appears that in some intervals of magnitude energy parameters are not affected by variations in the magnitude itself.

Table IX. Regression coefficients of the relative attenuation of design seismic hazard energy factor

R(AEI) DESIGN				
Magnitude	Soil	$\ln 1/K_2$	K_1	K_3
$6{\cdot}5 \leqslant M \leqslant 7{\cdot}1$	S1	0·5010	0·0182	0·5093
	S2	0·1423	0·0358	0·0783
	S3	0·1545	0·0175	0·1201
$5{\cdot}4 \leqslant M \leqslant 6{\cdot}2$	S1	0·9085	0·0009	0·9865
	S2	0·5366	0·0195	0·5627
	S3	0·4638	0·0136	0·4497
$4{\cdot}2 \leqslant M \leqslant 5{\cdot}2$	S1	0·5013	0·0070	0·6146
	S2	0·7269	0·0116	0·7572
	S3	0·5785	0·0072	0·5999

Consequently, it has been considered correct to select the four intervals of magnitude in the definition of the design spectra in terms of energy.

Although the constituted data set is the most extended among those employed in studies related with seismic input energy, the possibility that the previous assertion might result from either the natural limitations of the examined case-histories or the influence of factors difficult to quantify at present cannot be excluded. The discontinuous trend mentioned above could obviously exert a considerable effect on the usual seismic hazard analysis based on the frequency–magnitude relation. The recent Kobe (1995) and Northridge (1994) earthquakes have revealed that, though in the presence of a magnitude not particularly high, the Seismic Input energy has reached extremely high values[16] in close proximity to the source. Therefore, from this point of view the distance from the source factor acquires a primary and decisive meaning. Indeed, even with different extensions, earthquakes of magnitude within a specified interval may produce equivalent effects in the epicentral area.

As far as the *near-field* is concerned, it seems appropriate to introduce an interval of distance close to the source, ranging from 0 to 5 km, within which it is possible to suppose that the energy parameters assume maximum constant values. This hypothesis appears justified when both the unavoidable uncertainty in the definition of the distance from the source and the trend resulting from the analysis of the available data as a whole are considered.

The size and attenuation of the energy parameters depend significantly on the soil class, whose consideration reduces dispersions, thus allowing a more adequate identification and interpretation of the observed trends. For a fixed distance from the source, the Seismic Input Energy displays a definite tendency to increase as the soil stiffness decreases. In other words, the higher values of the energy parameters correspond to soil S3. Though this behavior is general, the relative dimensions of the parameters corresponding to the three types of soil vary with the considered intervals of magnitude and distance.

11. ELASTIC DESIGN EARTHQUAKE INPUT ENERGY SPECTRA

Once the spectral shapes and the energy seismic hazard energy factor have been defined, it is possible to obtain the design input energy spectra (Figure 5) as follows:

$$E_{\mathrm{I}}(T_i) = f_{\mathrm{E}}(T_i) \times \text{seismic hazard energy factor} \rightarrow E_{\mathrm{I}}(T_i) = f_{\mathrm{E}}(T_i) \times \mathrm{AEI(0\text{-}4)} \tag{12}$$

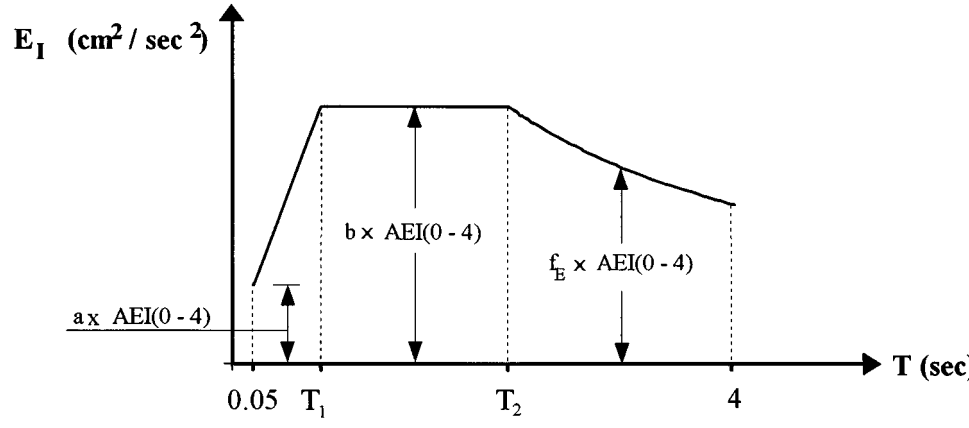

Figure 5. Linear elastic design earthquake input energy spectrum

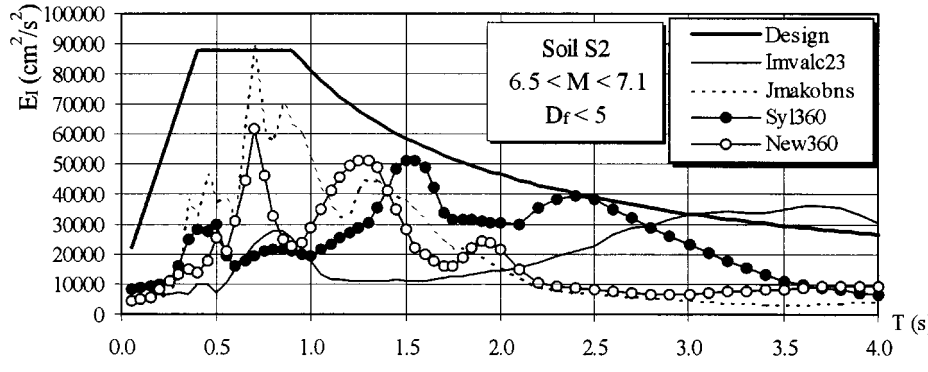

Figure 6. Comparison of the design elastic E_I spectra and those relative to the most significant records. Soil S2

where $E_I(\mathrm{cm}^2/\mathrm{s}^2)$ represents the energy per unit mass imparted to a structure of period T_i, $f_E(\mathrm{s}^{-1})$ is the normalized spectral ordinate as a function of the soil type corresponding to the same period T_i, and AEI(0-4) $(\mathrm{cm}^2/\mathrm{s})$ is the Seismic Hazard Energy Factor that depends on the magnitude interval and the source-to-site distance interval.

Finally, the following functional relationship can be written:

$$E_I(T_i) = f(T_i, S, M, D_f, \xi) \tag{13}$$

where T_i is the vibration period of the structure, S is the soil type, M is the magnitude interval, D_f is the source-to-site distance interval, and ξ is the viscous damping coefficient, assumed equal to 5 per cent of the critical value.

In Figure 6 the design input energy spectrum for the soil S2, the magnitude interval 6·5–7·1, and the source-to-site distance interval 0–5 km, is compared with the input energy spectra corresponding to the most significant strong ground motion records for this type of soil (El Centro, #7 Imperial Valley College 230 comp., Imperial Valley Earthquake, 1979; Kobe JMA NS comp., Kobe Earthquake, 1995; Sylmar County

Hospital Parking lot 360 comp., and Newhall LA County Fire Station 360 comp., corresponding to the Northridge Earthquake 1994).

Finally, although the probability that the design input energy spectra is exceeded depends on the vibration period and the considered class (Magnitude interval, distance D_f interval, soil type), it is possible to assume on average that it corresponds to a percentile of 65 per cent.

12. CONCLUSION

(1) The analyses carried out have led to a proposal of design spectral shapes as a function of the soil type. Similar shapes are described with simple mathematical expressions, using parameters depending on the type of soil. The spectral shapes are converted in design seismic input energy spectra using a scale factor defined as the seismic hazard energy factor, which constitutes an adequate index for the characterization of the earthquake damage potential.

(2) The amount of energy at the source and the modality of the release (i.e. magnitude and rupture process) significantly affect the intensity and the variation with T_i of the seismic input energy. Although the seismic input energy increases with the magnitude, the seismic hazard energy factor increase with magnitude but in a *discontinuous* manner, as no significant variation in either the maximum input energy and the area of the spectrum are observed within certain intervals of magnitude.

(3) The type of soil where the records have been obtained has a significant influence on the evaluation of the input energy.

(4) The attenuation of the seismic input energy with distance from the source of an event, evaluated using either the maximum input energy, E_I(max), or AEI(0-4), displays a trend completely different from those of PGA and PGV.

(5) Recent earthquakes with magnitude 6·8–7·0, have shown extremely high values of the seismic energy input in the proximity of the source indicating that urban centres localized near seismotectonic structures capable of generating events of such dimensions are exposed to high seismic risks. Therefore, it would be necessary to revise the present criteria of evaluate seismic hazards in a given site.

REFERENCES

1. G. W. Housner, 'Limit design of structures to resist earthquakes', *Proc. Ist WCEE, Berkeley, California*, 1956 pp 5.1–5.13.
2. T. Zahrah, and J. Hall, 'Earthquake energy absorption in SDOF structures', *J. Struct. Div. ASCE*, **8**, 1984.
3. H. Akiyama, *Earthquake Resistant Limit-state Design for Buildings*, University of Tokyo Press. Japan, 1985.
4. C. M. Uang, and V. V. Bertero, 'Use of energy as a design criterion in earthquake resistant design', *Report No. UCB/EERC*-88/18, Earthquake Engineering Research Center, University of California at Berkeley, 1988b.
5. P. Fajfar, T. Vidic and M. Fishinger, 'Seismic demand in medium and long-period structures', *Earthquake Engng. Struct. Dyn.* **18**, 1133–1144 (1989).
6. P. Fajfar, and T. Vidic, 'Consistent inelastic design spectra: hysteretic and input energy', *Earthquake Engng. Struct. Dyn.* **23**, 523–532 (1994).
7. A. A. Nassar and H. Krawinkler, '*Seismic demands for SDOF and MDOF systems*', *Report No. 95,* John A. Blume Earthquake Engineering Center, Department of Civil Engineering, Stanford University, California (1991).
8. R. S. Lawson, and H. Krawinkler, 'Cumulative damage potential of seismic ground motion', in Duma (ed), 10th European Conference on Earthquake Engineering, 1995 Balkema, Wien, pp. 1079–1086.
9. V. V. Bertero, 'Lesson learned from recent catastrophic earthquake and associated research', *First Torroja Int. Lecture*, ICCET, 1989.
10. C. M. Uang, and V. V. Bertero 'Implications of recorded earthquake ground motions on seismic design of buildings structures, *Report No. UCB/EERC-88/13*, Earthquake Engineering Research Center, University of California at Berkeley 1988a.
11. F. Mollaioli, 'Formulazione energetica del potere distruttivo dei terremoti. Analisi alla sorgente, propagazione, effetti locali e risposta strutturale', Tesi di Dottorato di Ricerca in Ingegneria delle Strutture, Università di Roma "La Sapienza", Roma, Febbraio 1996 (in Italian).
12. H. Kuwamura, and T. V. Galambos, 'Earthquake load for structural reliability', *J. Struct. Engng.* ASCE, **115**, 1446, 1462 (1989).
13. R. C. Riddell, Espectros de energia disipada y daño sismico. *MEM. 5as. Jorn. Chilenas de Sismologia e Ing Antisismica, Santiago, Chile* **2**, 895–904, 7–11 August, 1989

14. P. Fajfar, T. Vidic and M. Fishinger, On energy demand and supply in SDOF systems. In: *Nonlinear Seismic Analysis and Design of RC Buildings* ed. P. Fajfar and H. Krawinkler, Elsevier Applied Science, pp. 41–61.
15. V. V. Bertero, R. A. Herrera and S. A. Mahin, Aseismic design implications of near-fault San Fernando Earthquake records. *Earthquake Engng. Struct. Dyn.* **6**, 31–42 (1978).
16. L. D. Decanini, and F. Mollaioli, Il Terremoto di Kobe del 1995: danneggiamenti osservati su edifici e correlazione con linput sismico. 7°*Convegno Nazionale*: *L'ingegneria sismica in Italia*, *Siena*, 1995.
17. H. Sucuoglu and A. Nurtug, Earthquake ground motion characteristics and seismic energy dissipation. *Earthquake Engineering and Structural Dynamics* **24**, 1159–1213 (1995a).
18. W. B. Joyner, and D. M. Boore, Peak horizontal acceleration and velocity from strong motion records including records from the 1979 Imperial Valley, California, Earthquake. *Bulletin of Seismological Society of America* **71**, 2011–2038 (1981).
19. N. Ambraseys, Intensity-attenuation and magnitude-intensity relationships for Northwest European earthquakes. *Earthquake Engng. and Struct. Dyn.* **13**, 733–778.

